P. Adkin and S. J. Harvey**

On Buckling and Deformation Modes of Tubes Subject to Cyclic Plasticity

REFERENCE Adkin, P. and Harvey, S. J., **On buckling and deformation modes of tubes subject to cyclic plasticity**, *Biaxial and Multiaxial Fatigue*, EGF 3 (Edited by M. W. Brown and K. J. Miller), 1989, Mechanical Engineering Publications, London, pp. 173–184.

ABSTRACT The buckling behaviour of thin walled tubes subjected to (i) monotonic compression and (ii) cyclic plastic push–pull loading, both with and without internal pressure, has been investigated experimentally. A theoretical analysis predicts that longitudinal and circumferential bending moments are induced by the additional internal pressure, and the experimental results show that buckling is more pronounced when an internal pressure is present. The hoop strains, resulting from the application of internal pressure show waveforms consistent with the buckling effect in the compression cycle.

Theoretical prediction of the internal pressures required for given strain ratios compare well with measured data. Test results in cyclic push–pull without internal pressure also indicate that a kinematic hardening model is representative of cyclic material behaviour.

Introduction

Many experimental procedures to obtain verification of plastic flow rules and yield surface data are based on tests with thin walled tubular specimens subjected to a range of loading conditions, being predominately in torsion–tension, or axial tension with internal pressure. A vast amount of experimental data is available concerning the shape of the yield surfaces, the presence or absence of corners in the yield surface, cross-hardening effects, anisotropy, and flow rules.

Adequate testing procedures have been developed for monotonic loading conditions, particularly when the plastic strains are small. However, buckling problems can arise when the plastic strains are increased, particularly with compressive and torsional loads, and this buckling problem is exacerbated when cyclic loads are applied. Torsional buckling has often been observed at quite small plastic cyclic strains and solid inserts are often placed inside the tube to limit the buckling. One method of reducing the buckling is to increase the specimen thickness, but this leads to stress gradients and the loss of plane stress conditions. The problem of buckling of thin walled tubes under axial compression has been widely investigated, and Florence and Goodier (**1**) developed a solution which related the buckling modes with bending moments induced during the unperturbed displacements of the specimen. The theory developed was similar to that for the plastic buckling of cylindrical shells under external radial impulse loads (**2**).

* Lanchester Polytechnic, Coventry, UK.

In many cyclic plasticity problems strain accumulation or ratchetting can occur and test data are required in order to evaluate appropriate yield criteria and flow rules. The presence of buckling makes experimental data unreliable and the purpose of this research was to examine the buckling and deformation modes of thin walled tubes in (i) direct compression, (ii) cyclic push–pull, and (iii) cyclic push–pull with a sustained internal pressure. Based on the results obtained it was hoped that test procedures could be determined and specimen design optimised in order to reduce buckling to an acceptable level and therefore provide reliable cyclic material data.

Notation

$\sigma_r', \sigma_\theta', \sigma_z'$	Deviatoric stresses in radial, hoop, and axial directions, respectively
$\varepsilon_r, \varepsilon_\theta, \varepsilon_z$	Plastic strains in radial, hoop, and axial directions, respectively
k	Shear yield stress
r	Radius
b	External radius
C	Parameter dependent on relative rates of expansion and extension
u, w	Radial and axial displacements, respectively
l	Gauge length
M_z, M_θ	Axial and circumferential bending moments, respectively

A dot signifies rate derivative, e.g., $\dot{l}$

Theoretical considerations

The general solution for a tube subjected to tension or compression with internal pressure has been given by Hill (**3**).

He showed that for transverse sections to remain plane the axial and radial displacements are given by

$$u = \frac{-\dot{l}r}{2l} + \frac{C}{r}, \qquad \omega = \frac{\dot{l}z}{l}$$

The incompressibility equation gives

$$\frac{\partial u/\mathrm{d}r}{u/r} = \frac{(-\dot{l}/2l) - (C/r^2)}{-(\dot{l}/2l) + C/r^2} = \frac{\sigma_r'}{\sigma_\theta'}$$

Substituting into the yield condition

$$\sigma_r'^2 + \sigma_r'\sigma_\theta' + \sigma_\theta'^2 = k^2$$

we obtain

$$\frac{\sigma_r'}{k} = -\frac{[1 + \{(\dot{l}r^2)/(2lC)\}]}{[1 + \{(3\dot{l}^2r^4)/(4l^2C^2)\}]^{1/2}} \qquad \text{and}$$

$$\frac{\sigma_\theta'}{k} = \frac{[1 - \{(\dot{l}r^2)/(2lC)\}]}{[1 + \{3\dot{l}^2r^4)/(4l^2C^2)\}]^{1/2}}$$

The axial stress is given by

$$\frac{\sigma_z}{k} = \frac{\sigma_r - (2\sigma'_r + \sigma'_\theta)}{k}$$

which reduces to

$$\frac{\sigma_z}{k} = \frac{[1 + \{(3\dot{l}r^2)/(2lC)\}]}{[1 + \{(3\dot{l}r^4)/(4l^2C^2)\}]} - \coth^{-1}\sqrt{[1 + \{(3\dot{l}^2r^4)/(4l^2C^2)\}]} + \coth^{-1}\sqrt{[1 + \{(3\dot{l}^2b^4)/(4l^2C^2)\}]}$$

Now, when there is no internal pressure, $C = 0$, and we have a uniform stress across the wall thickness. However, when an internal pressure is applied, we obtain not only a variation in σ_θ, but also a variation in σ_z through the thickness. This means that the internal pressure induces moments M_z and M_θ throughout the specimen. Hills solution differs from that of Florence and Goodier (1) because they assumed a strain distribution in simple compression which automatically led to stresses being predicted and, consequently, through the yield criterion, variations in the longitudinal stress. If we follow Hills solution through and select particular strain conditions we can show that it is the introduction of the internal pressure which produces the longitudinal moment, M_z. Theoretically, therefore, in simple compression we would not expect any moments to be induced which might aid the buckling process. However, localised moments will be introduced at the shoulders of the specimen (the blend radii), but these should diminish as we move along the gauge length. These end constraints will be more pronounced for large axial strains and the introduction of internal pressure will generate moments which may assist the buckling process.

Materials, specimens, and test procedure

The materials used in this investigation were a low carbon steel (EN32m) and a stainless steel (AISI 321). They had the following elemental composition (percentages by weight).

Material	*C*	*Si*	*Mn*	*S*	*P*	*Ni*	*Cr*	*Mo*	*Ti*
AISI 321	0.05	0.25	1.79	0.008	0.03	10.26	17.82	–	0.61
EN 32m	0.18	0.05	0.04	0.9	0.11	–	–	–	–

The general shape of the test specimen is shown in Fig. 1(a), where the blend radius into the gauge length was varied in order to determine the optimum radius to minimize buckling. Large blend radii have often been used to reduce the stress concentrations which would cause fatigue failure, but this can lead to unwanted triaxial stresses.

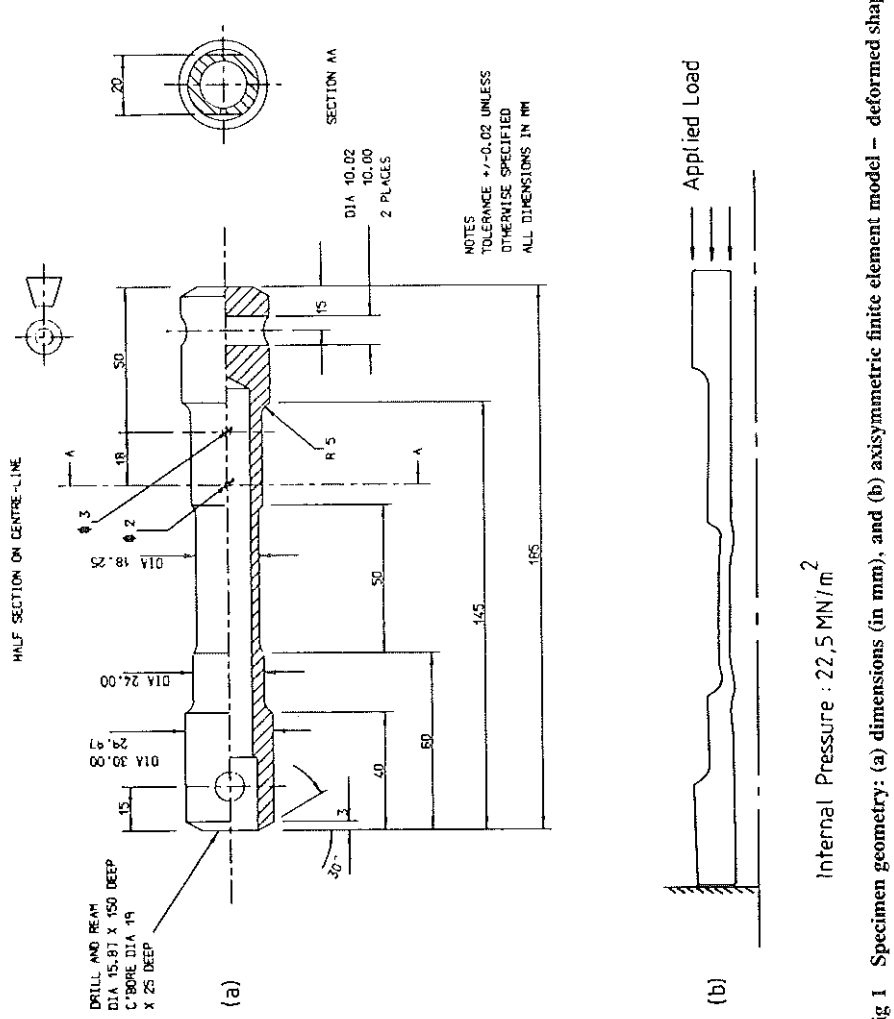

Fig 1 Specimen geometry: (a) dimensions (in mm), and (b) axisymmetric finite element model – deformed shape

Axial strains were measured by a gauging LVDT, mounted via a perspex clamp, on one shoulder of the specimen. A second perspex block was clamped to the other shoulder of the specimen and acted as the LVDT striker plate. Two diametral marks were also scribed on the central portion of the specimen 25.40 mm apart in order to determine the local strain in this region. The specimen profiles, shoulder-to-shoulder gauge length, and scribed gauge length, were measured before and after testing using a toolmaker's microscope which had a resolution of 0.00127 mm. Four blend radii of 3, 5, 10, and 15 mm were used with internal pressures up to 22.5 MN/m^2. The test machine and data acquisition system are fully described elsewhere (**4**). Special care was taken to ensure no bending stresses were introduced due to any misalignment during the loading process.

The compressive loads were applied hydraulically to give a 3 per cent total strain between the specimen shoulders. The internal pressure insert was designed to ensure that there was adequate clearance between the specimen wall and the insert during all tests.

Initial finite element analysis had shown that, even for elastic deformation, buckling would be induced due to the constraints at the shoulder of the specimen and a typical deformation mode is shown in Fig. 1(b). Without these constraints a uniform expansion is predicted by the finite element method for the case of a tube loaded in simple compression.

Results

The waveforms developed for the different blend radii following a nominal 3 per cent compression strain are shown in Fig. 2, for the AISI 321 material and similar results were obtained for the EN32m material.

With a 3 mm blend radius we can see, in Fig. 2(a), the effects of the end constraints, but there is a fairly parallel central portion. With the 5, 10, and 15 mm blend radii we can observe an extra waveform being developed. However, the buckling over the central portion was considerably reduced for lower strains and was barely detectable over the central portion of the gauge length when cycling at ± 1 per cent total strain for 30 cycles. The introduction of an internal pressure increased the buckling and this is shown in Fig. 3 which gives the profile after cycling 1 per cent total strain for 15 cycles with an internal pressure of 22.5 MN/m^2.

In addition to quantifying the buckling, it is important that the strain over the gauge length be accurately measured and recorded. Strains were measured between the shoulders of the specimen, a 50 mm gauge length, and also over a central 25 mm gauge length. The strains actually recorded for an apparent 3 per cent compressive strain between the shoulders of the specimen are shown in Table 1. It can be seen that the development of buckling can lead to significant errors in recording the true strain and that the measurements of strain and strain monitoring during cycling should be restricted to as small a gauge length

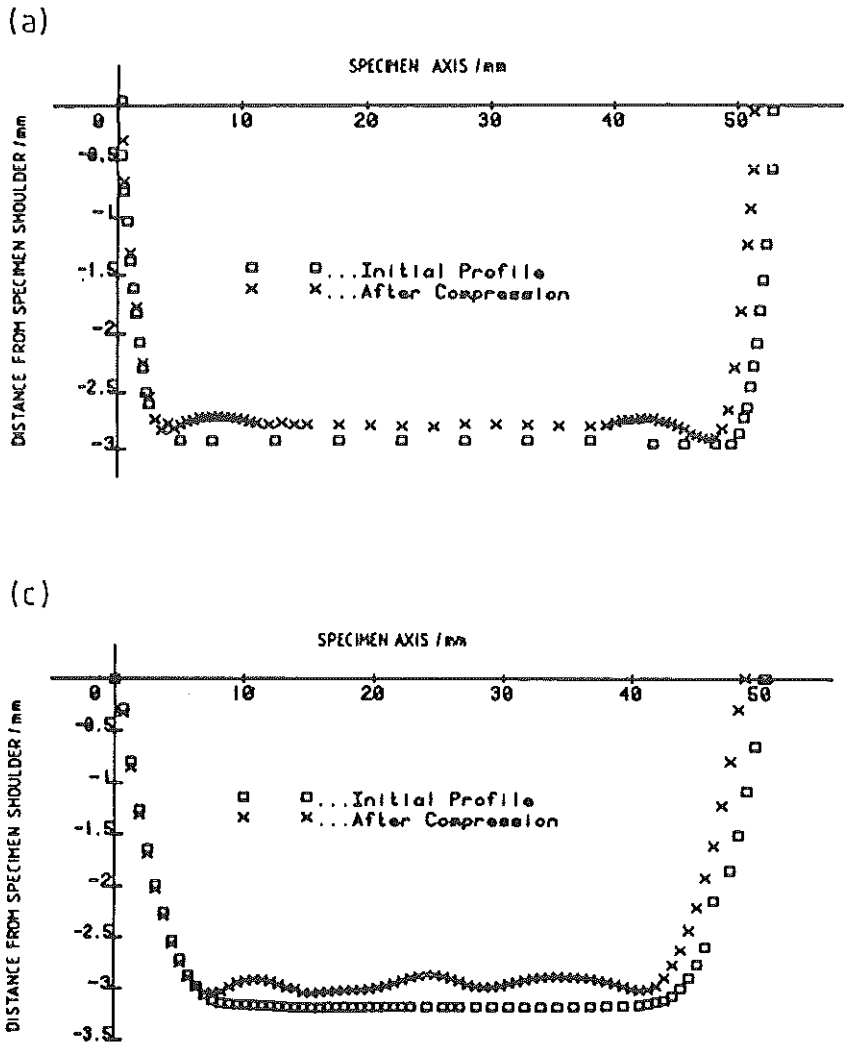

Fig 2 Specimen profiles after 3 per cent monotonic compression: (a) 3 mm radius; (b) 5 mm radius; (c) 10 mm radius; (d) 15 mm radius

(b)

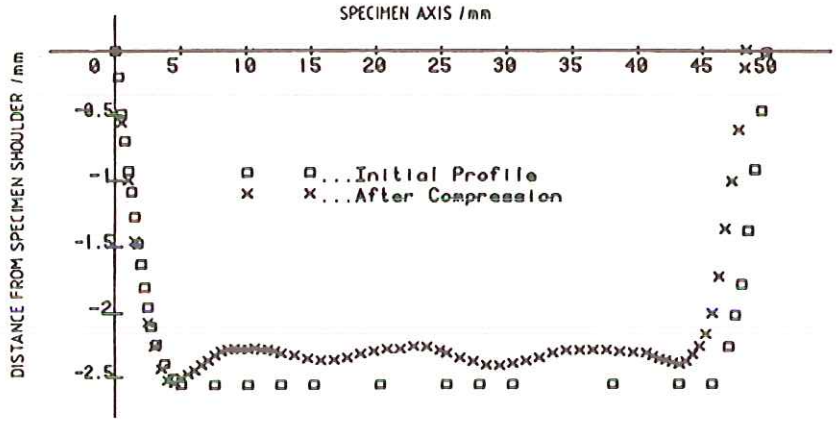
SPECIMEN AXIS /mm
0
5
10
15
20
25
30
35
40
45
x50
DISTANCE FROM SPECIMEN SHOULDER /mm
-0.5
-1
-1.5
-2
-2.5
□...Initial Profile
×...After Compression

(d)

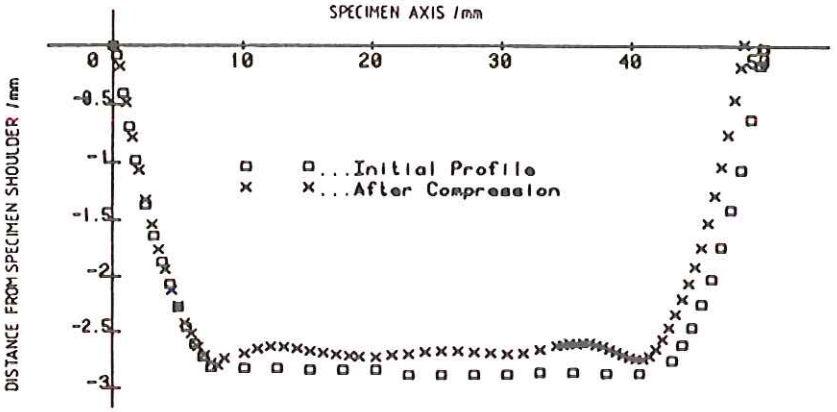
SPECIMEN AXIS /mm
0
10
20
30
40
DISTANCE FROM SPECIMEN SHOULDER /mm
-0.5
-1
-1.5
-2
-2.5
-3
□...Initial Profile
×...After Compression

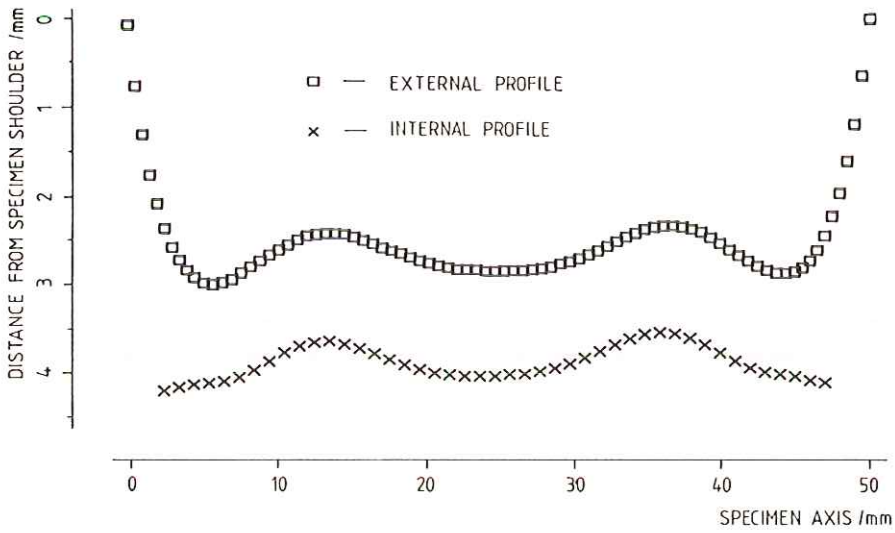

Fig 3 Specimen profile following 15 cycles at 1 per cent total axial strain. Internal pressure = 22.5 MN/m²; material – AISI 321

as possible in the central portion of the specimen, and strain control between the shoulders avoided. As a result of a large number of tests it was decided that, although the apparent buckling was less for the 3 mm blend radius, the strain measurement over the centre of the gauge length was equally good for the 5 mm blend radius. Therefore, in order to minimize the stress concentration at the shoulder and its consequent effects on fatigue life a 5 mm blend radius was chosen for cyclic strains up to ±1.0 per cent.

The buckling effects can be detected when measuring the hoop strains during a cycle of push–pull and, again, the effect of internal pressure is noticeable in the hoop strain characteristic. The slight waveform on the compressive cycle can be seen in Fig. 4 for cyclic strains of ±1 per cent and an internal pressure of 22.5 MN/m² for the low carbon steel (EN32m). At lower pressures this waviness is absent, as shown in Fig. 5(a) for an internal pressure of 8.54 MN/m².

Table 1 Experimental strain measurements

Specimen blend radius (mm)	*Plastic strain (whole gauge length) – optical (1) 50 mm*	*Plastic strain (scribed gauge length) – optical (2) 25 mm*	*Plastic strain (whole gauge length) – LVDT*	*Percentage error* $\frac{(2)-(1)\times 100}{(1)}$
3	0.02789	0.03221	0.02829	13.41
5	0.02930	0.03404	0.03020	13.92
10	0.02883	0.03614	0.02960	28.61
15	0.02772	0.04302	0.02797	35.56

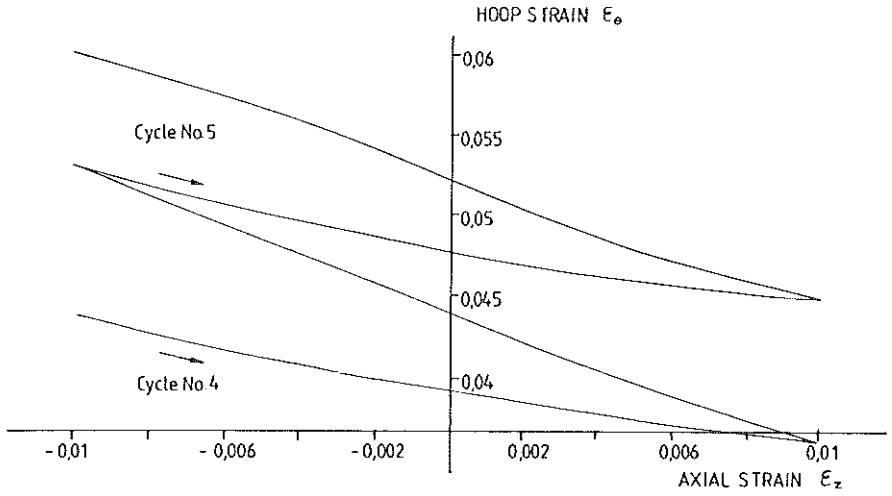

Fig 4 Hoop strains for large internal pressure (22.5 MN/m²)

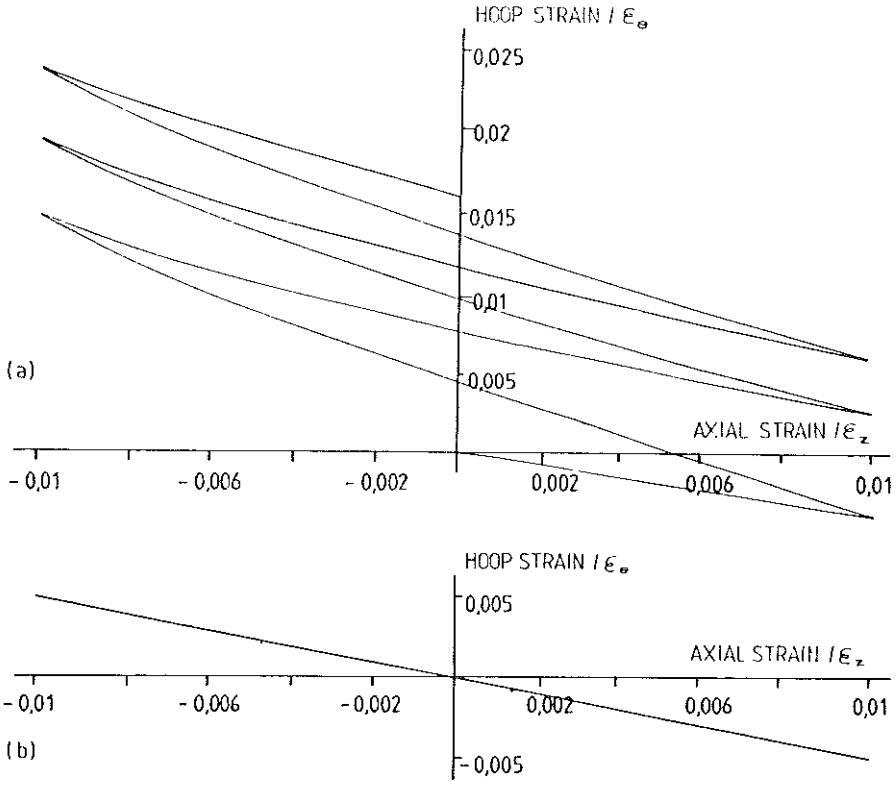

Fig 5 Hoop strains for: (a) small internal pressure (8.54 MN/m²), and (b) no internal pressure

When cycling without internal pressure the ratio of hoop strain to axial strain is $-\frac{1}{2}$, as shown in Fig. 5(b).

Discussion

In order to examine the validity of the Hill method the stresses were calculated for five loading conditions using monotonic material data. The test conditions are given in Table 2.

It is possible to compare the predicted axial stress and internal pressure with measured values for the particular strains, using values of k obtained from uniaxial tests at the appropriate equivalent strain. Given the complexity of the problem it is felt that the theoretical predictions are good.

The axial stress distributions are shown in Fig. 6 and Fig. 7. It can be seen that the axial stress is practically uniform for very small internal pressures. The generally good agreement obtained gives confidence in the theoretical approach and tends to confirm that no longitudinal or circumferential moments are induced by simple compressions as previously assumed (**1**), except those due to end effects in the region of the blend radius.

A comprehensive series of tests involving unloading at various stages in the cyclic process for both uniaxial and biaxial stress states was undertaken (**4**), and it was concluded that, in the steady state condition, a kinematic hardening model adequately described the cyclic material behaviour for both the low carbon steel and the stainless steel. In addition to this, the fact that the ratio of plastic hoop strains to plastic axial strain remained $-\frac{1}{2}$ during cycling, (Fig. 5(a)) would result in a kinematic yield surface which moves in a direction parallel to the σ_2 axis, which is consistent with the model of Ziegler (**5**) and was previously discussed with reference to cyclic plasticity problems by Hancell and Harvey (**6**), see Fig. 8.

Conclusions

The application of internal pressures when tubes are subjected to cyclic plastic push–pull strain induces longitudinal as well as circumferential bending moments. These moments appear to assist the buckling process, and, although

Table 2 Comparison of theoretical and experimental data for EN32m

				Applied	*Calculated*	*Applied*	*Calculated mean*
Case	ε_z	ε_θ	k (MN/m^2)	σ_r	σ_r	σ_z	σ_z
A	0.002	−0.001	137	0	0	–	–
B	0.002	−0.00056	139	−8.54	−8.25	255	265
A1	−0.002	0.001	137	0	0	–	–
B1	−0.002	0.00144	139	−8.54	−8.25	–	–
C	−0.002	7.7 × 10	154	−22.5	−21.3	306	299

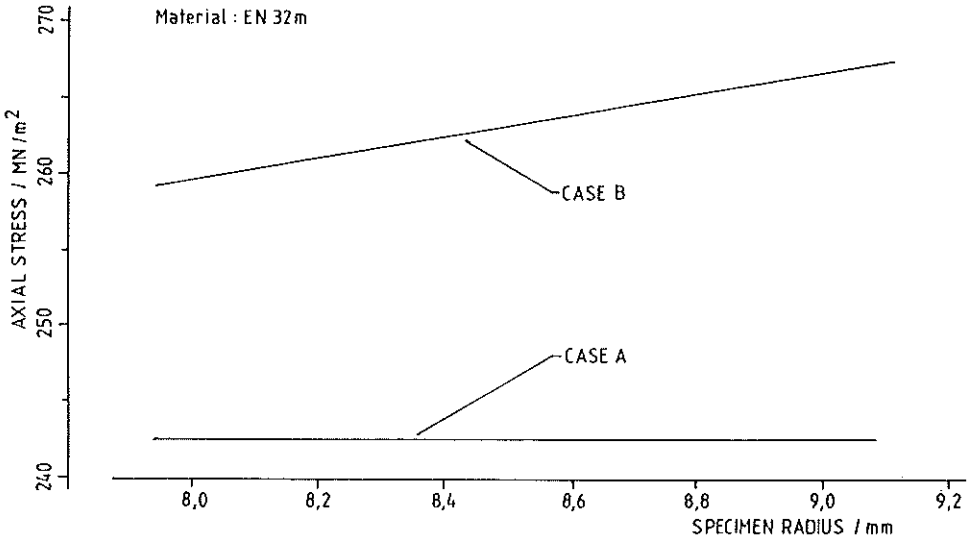

Fig 6 Predicted stresses on the tension stroke: Case A = low internal pressure; Case B = high internal pressure

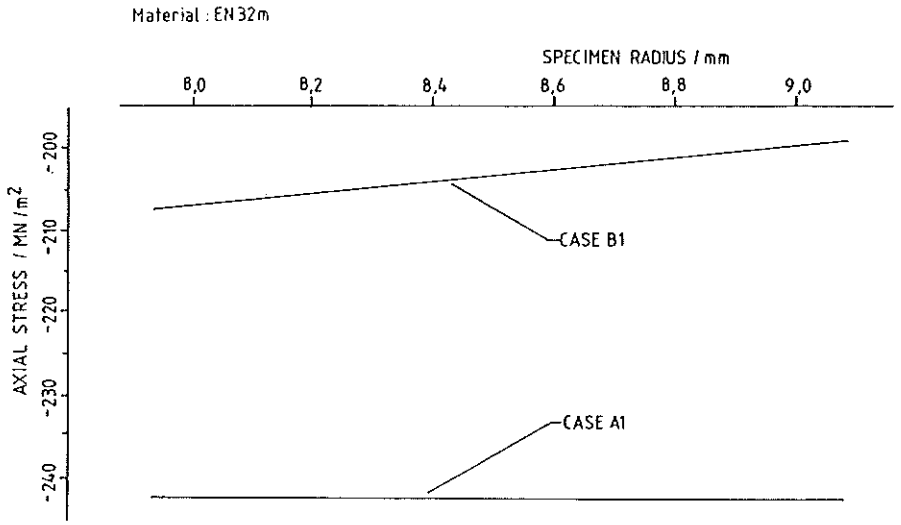

Fig 7 Predicted stress on the compression stroke: Case A1 = low internal pressure; Case B1 = high internal pressure

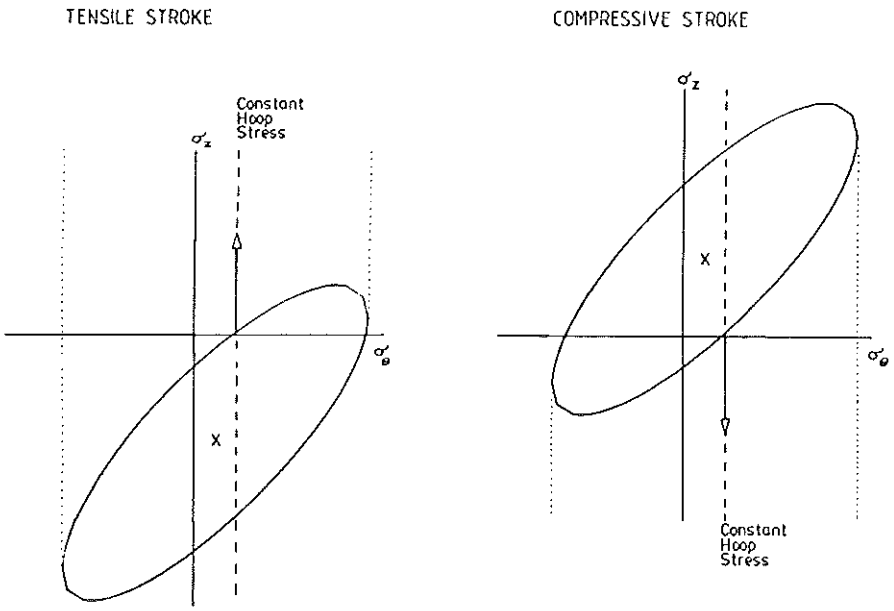

Fig 8 Kinematic hardening model at steady state cyclic loading conditions (push–pull)

the buckling effect can be minimized by restricting the cyclic strains and employing good testing procedures, its presence should not be ignored.

A kinematic hardening model is consistent with the cyclic material behaviour observed and the strain pattern obtained without internal pressure. This model can form the basis for calculating the ratchetting hoop strain when a sustained internal pressure is applied (**4**).

References

(1) FLORENCE, A. L. and GOODIER, J. N. (1968) Dynamic plastic buckling of cylindrical shells in sustained axial compressive flow, *J. Appl. Mech.*, **35**, 80–86.
(2) ABRAHAMSON, G. R. and GOODIER, J. N. (1962) Dynamic plastic flow buckling of a cylindrical shell from uniform radial impulse, *Proc. 4th U.S. National Congress of Applied Mech., ASME*, pp. 939–950.
(3) HILL, R. (1956) *The mathematical theory of plasticity*. Oxford University Press, Oxford.
(4) ADKIN, P. (1986) *Yield surfaces in cyclic plasticity*, PhD thesis, Coventry Polytechnic.
(5) ZIEGLER, H. (1959) A modification of Pragers hardening rule, *Q. Appl. Mech.*, **17**, 1–26.
(6) HANCELL, P. J. and HARVEY, S. J. (1979) The use of kinematic hardening models in multi-axial cyclic plasticity, *Fatigue Engng Mater. Structures*, **1**, 271–279.